The First Two Host Galaxies of X-ray Flashes: XRF 011030 and XRF 020427

J. S. Bloom[1,2], D. Fox[3], P. G. van Dokkum[4], S. R. Kulkarni[3], E. Berger[3], S. G. Djorgovski[3], and D. A. Frail[5]

[1] *Harvard-Smithsonian Center for Astrophysics, MC 20, 60 Garden Street, Cambridge, MA 02138, USA*

[2] *Harvard Society of Fellows, 78 Mount Auburn Street, Cambridge, MA 02138, USA*

[3] *Palomar Observatory 105–24, California Institute of Technology, Pasadena, CA 91125, USA*

[4] *Department of Astronomy, Yale University, New Haven, CT 06520-8101, USA*

[5] *National Radio Astronomy Observatory, Socorro, NM 87801, USA*

ABSTRACT

Given the paucity of empirical constraints, the nature of the newly-recognized phenomena called X-Ray Flashes (XRFs) has been an open question. However, with the recent detections of radio and X-ray afterglow it is finally possible to study the large- and small-scale environments of XRFs. We present *Chandra*, *Hubble Space Telescope* (HST), and Keck observations of the fields of XRFs 011030 and 020427. Astrometric comparisons of the X-ray transient positions and the HST images reveal the XRFs to be associated with faint blue galaxies. Photometric evidence of these putative hosts suggests that these two XRFs originated from redshifts less than $z \sim 3.5$, and thus cannot be due to GRBs at very high redshifts. In both host–burst offsets and host properties, these XRFs could have been drawn from distributions similar to those measured of gamma-ray bursts (GRBs). We conclude with a discussion of the implications of this XRF–GRB host connection for the possible progenitors of XRFs.

Subject headings: gamma rays: bursts — X rays: bursts

1. Introduction

A new class of high energy transients called X-ray Flashes (XRFs) has been identified (see Heise et al. 2003 and Yamazaki et al. 2003 for recent reviews). These events have an

annual all-sky rate which is between one third to one half of the gamma-ray burst (GRB) rate and thus make a substantial contribution to the cosmic explosion rate. In many respects, particularly in their duration, the *prompt* burst properties of XRFs overlap with those of the class of long duration gamma-ray bursts. Within the statistics limited by the small number of identified events, about 30 thus far, XRFs appear to be isotropic and inhomogeneous, suggestive of a cosmological distribution (as with GRBs). However, the principal difference, as connoted by the nomenclature is that the bulk of the energy of XRFs is measured in the X-ray band, with a peak energy E_p below roughly 50 keV (Kippen et al. 2001; Barraud et al. 2003). In contrast, in the extensive sample of GRBs detected by *BATSE*, E_p is clustered around 200 keV with a distinct roll-off toward lower values of E_p (e.g., Preece et al. 2000).

The discovery of X-ray (Harrison et al. 2001; Amati et al. 2002) and radio (Taylor et al. 2001) afterglows are consistent with XRFs being of cosmological origin (Heise et al. 2003). However, whereas at least some long-duration GRBs are a result of the death of massive stars (see Bloom 2003 for review), the physical mechanism(s) responsible for the production of XRFs is completely unknown. Theoretical models for the origin of XRFs have been explicated elsewhere (Yamazaki et al. 2002; Woosley et al. 2002; Zhang & Mészáros 2002; Barraud et al. 2003; Mochkovitch et al. 2003). To summarize, XRFs could arise from a new physical class of explosions, GRBs which originate from very large redshifts ($z \gtrsim 6$; Heise et al. 2001), or lower-redshift variants of GRBs (e.g., GRBs beamed away from Earth: Yamazaki et al. 2002, GRBs with dense ambient gas, or transition GRBs with lower Lorentz factor outflows: Dermer et al. 1999). To our knowledge, the only reason to possibly associate XRFs with the death of massive stars is that XRFs appear to have a duration distribution similar to those of the long-duration GRBs.

A basic discriminator of the various XRF progenitor models is a measurement of the distance to the explosions. In the absence of a direct redshift measurement, it is possible to constrain the distance by examining photometric and morphological properties of the host galaxies of XRFs. Irrespective of the redshifts, the nature of the hosts themselves and the location of XRFs within their hosts, in analogy with GRBs, will play an important role in understanding the progenitors. Here we report on the host galaxies of the first two XRFs with sub-arcsecond afterglow localizations[1]. In both cases, we identify a putative host galaxy. Here we present accurate astrometry of the XRFs and describe the properties of the hosts. Finally, we compare the properties of the host galaxies of GRBs and find that the XRF host

---

[1]At least one additional XRF has been subsequently localized to a sub-arcsecond position. Fox et al. (2003) discovered the apparent optical/IR afterglow of XRF 030723 (Prigozhin et al. 2003). Soderberg et al. (2002) found a possible optical transient of XRF 020903, which was associated with a low redshift star forming galaxy ($z = 0.25$).

galaxies are quite similar to those of GRB galaxies, namely typical star forming galaxies at moderate redshifts. The discoveries of the hosts discussed herein have been previously announced (XRF 011030: Fruchter et al. 2002; XRF 020427: Castro-Tirado et al. 2002).

2. Observations and Reduction

Our X-ray observations with the *AXAF CCD Imaging Spectrometer* (ACIS) on-board the *Chandra* X-ray Observatory (CXO) were first reported in Harrison et al. (2001) for XRF 011030 and in Fox (2002b) and Fox (2002a) for XRF 020427. The data were reduced and analyzed using the *CIAO* software package[2]. The X-ray afterglow of XRF 011030 was identified by Harrison et al. (2001) in a 47 ksec exposure beginning on 2001 Nov 9.73 UT, consistent with the radio transient position (Taylor et al. 2001). A second 20 ksec epoch was obtained on 2001 Nov 29.44 UT. The sub-arcsecond location of the X-ray afterglow of XRF 020427 (Amati et al. 2002) was identified in the CXO imaging as a fading point source between two CXO pointings (beginning 2002 May 6.24 UT: 13.8 ksec and 2002 May 14.19 UT: 12.5 ksec). The fiducial absolute positions of the respective afterglow and field sources surrounding the XRFs were found using *CIAO*/Wavdetect.

For optical/IR imaging, the field of XRF 011030 (in 't Zand et al. 2001) was observed starting on 12.19 December 2001 UT as part of the Cycle 9 *HST* observing program GO 8588 (A. Fruchter, P.I.; see Fruchter et al. 2002). The field of XRF 020427 (in 't Zand et al. 2002) was observed starting on 14.62 June 2002 UT as part of our large Cycle 10 project GO 9180 (S. Kulkarni, P.I.). Both fields were observed in the STIS/50CCD ("Clear") and STIS/F28×50LP ("Longpass") filters. The image frames were retrieved from the STSCI archive after "On the Fly" preprocessing, where the raw data are pre-reduced using the best calibration data available at the time of retrieval. Individual exposures ranged from integrations of 864–1008 sec (XRF 011030) to 572–624 sec (XRF 020427). The total integration times were 8640 s and 9072 s (XRF 011030) and 4781 s and 4796 s (XRF 020427), for the Clear and Longpass filters respectively.

We combined the exposures and removed cosmic-rays using the standard methods outlined in IRAF/DRIZZLE2 (Fruchter & Hook 1997). Since few sources were detected in the Longpass images of XRF 020427, extra care was taken to remove cosmic rays before cross-correlating the exposures to find the relative offsets. In particular, we ran (for both filters) a Laplacian detection algorithm (LACOSMIC; van Dokkum 2001) on the images to detect and mask cosmic-rays before running the DRIZZLE routine PRECOR. In the XRF 011030

---

[2]See http://cxc.harvard.edu/ciao/

images, since several stars were saturated, we masked saturated pixels before performing the cross-correlation. The combined images were made using `drizzle.pixfrac`=0.7 and the final scale was 25.3 milliarcsec (mas) × 25.3 mas per pixel. In the drizzle process, images were rotated to cardinal orientation using the header information about the roll angles. We registered the images of the field in two filters using IRAF/CROSSCOR.

We also obtained supporting groundbased imaging of the XRF fields. For XRF 020427, three 600 s I-band exposures were taken using the *Wide Field Reimaging CCD Camera* at the Las Campanas Observatory (LCO) DuPont 100-inch telescope on 3 August 2002. After reductions, the images were registered and stacked yielding a $25' \times 25'$ final image centered on the XRF afterglow position. The effective seeing was $1.6''$ FWHM. On 24 December 2001 UT, we obtained 4500 sec of K_s-band imaging of the field of XRF 011030 using the NIRC instrument (Matthews & Soifer 1994) mounted on the Keck I 10 meter telescope in Mauna Kea, Hawaii. The zero-point of the combined image was determined from observations of four Persson et al. (1998) NIR standard stars, with an estimated zero-point uncertainty of 0.05 mag.

3. Astrometry: The location of the XRFs

3.1. XRF 011030

The HST STIS/Clear field includes apparent counterparts to three sources detected in our CXO imaging. An 11th magnitude star to the Southwest, which is the apparent counterpart of one of the CXO sources, is listed in the Tycho-2 catalog as TYC 4590-00070-1 ($d = 16.4 \pm 11.9$ pc, proper motion 100 ± 181 mas yr^{-1}, $V = 11.04$ mag; Hog et al. 2000). The other two objects, to the northeast in the STIS field, appear extended in the STIS/Clear image. However, we are reasonably confident that these sources provide a good astrometric tie since the first source appears to be a point-source superimposed on a galaxy and the other source has a smooth surface brightness profile and a well-defined center.

We centroided the HST and the CXO counterpart sources using a Gaussian-weighted fit. However, the Tycho-2 source is severely saturated in the HST image and so a direct centroiding proved difficult. Instead, we found the position of the HST source using the four diffraction spikes to find the intersection. The estimated error on this centering method is 30 mas (2 σ).

Comparing the nominal CXO and STIS/Clear spacecraft positions we require a shift of the CXO coordinates by 290 mas East and 60 mas South for the best fit. The uncertainty in this shift, taken as the mean of the standard deviation of the three offsets, is 80 mas

(2 σ). [Justified by the Tycho-2 measurements of the comparison stars, we assume that the proper motion/parallax between the XRF and HST epoch of the Tycho-2 source is significantly smaller that this r.m.s. scatter.] Since the uncertainty in the CXO coordinate shift is derived with only a few degrees of freedom, we consider this a systematic uncertainty. The internal (Poissonian) uncertainty in the CXO centroid of the XRF afterglow is 48 mas (2 σ). Adding the errors (not in quadrature), the conservative uncertainty radius for the XRF position on the STIS image is 128 mas (2 σ).

We have been able to make an independent registration of the CXO position by using the unified source catalog from VLA observations (Taylor et al. 2001). Four CXO sources, all distinct from the sources used for the STIS frame tie, have VLA counterparts. Correcting the CXO coordinates to the VLA frame (itself closely tied to the International Coordinate Reference Frame; ICRF) gives an adjustment of 230 ± 530 mas East, 120 ± 400 mas South, which is consistent with the HST adjustment we have made. Source positional uncertainties for this analysis are dominated by uncertainties in the radio centroiding, as the VLA data were taken in D-array (elliptical beamsize of 19.8×16.5 arcsec).

Identification of the Tycho star TYC 4590-00070-1 in the X-ray data, and confirmation of the roll angle and overall distortions by comparison with the HST and VLA data (see above) allows us to determine the absolute ICRF position of XRF 011030 with confidence. We find that the XRF afterglow is located at α(J2000)=$20^{\mathrm{h}}45^{\mathrm{m}}36^{\mathrm{s}}.007 \pm 0''.060$, δ(J2000) $= +78°06'01''.09 \pm 0''.066$. This $\sim$300 mas shift from the CXO position is entirely consistent with the absolute pointing accuracy (0.6'', 90% confidence) of *Chandra*[3].

An image depicting the position of the XRF on the HST image is shown in Figure 1. As noted previously (Fruchter et al. 2002), the XRF was located on the southeastern tip of a morphological irregular source, the probable host of XRF 011030. Following the methodology in Bloom et al. (2002), we measure the offset of the XRF to be 322±59 mas East, 106±65 mas South (offset distance $r = 339 \pm 60$ mas) of the apparent host center. No spectroscopic redshift is known for this galaxy. However, the offsets corresponds to 2.9 kpc in projection at a redshift of unity (using $H_0 = 65$ km s^{-1} Mpc^{-1}, $\Omega_m = 0.3$, $\Omega_\Lambda = 0.7$); since angular diameter distance is relatively insensitive to redshift over the range $z = 0.5$–5, this physical offset is expected to be accurate to $\sim$30 %.

---

[3]See http://cxc.harvard.edu/cal/ASPECT/celmon/.

3.2. XRF 020427

While one non-transient X-ray source falls on the STIS field, the nominal positions using the STIS and CXO headers did not coincide with any obvious STIS counterpart. An investigation of the guide star observation files, _jif, reveals that the STIS absolute pointing determined using two Guide Stars in the *Faint Guidance Sensors* (FGS) camera was suspect[4].

Instead of absolute astrometry, we registered both the HST and CXO frames independently to the LCO I-band image. We first found a world coordinate system for the LCO image using 298 GSC2.2[5] stars in the field. To tie the STIS WCS to the LCO image, we first re-sampled the STIS image by a factor of eight to 200 mas pixels. We then smoothed that image to one arcsec seeing and then re-sampled the LCO image to the same WCS zeropoint using IRAF/WREGISTER. Using IMALIGN and the 5 objects in common to both images, we then found a systematic shift of (1.041 ± 0.051) arcsec East, (1.320 ± 0.051) arcsec North between the native STIS and LCO WCSs.

To perform the CXO tie, we identified three stars in the LCO image with counterparts in the CXO data. Two of these stars are GSC 2.2 stars that were used to attach a WCS to the LCO image; for these purposes, however, we use their positions as derived from the image itself. The third tie object is the Tycho star TYC 9123-1224-1; this star was saturated in the LCO image and was not used to establish the WCS; for CXO astrometry we use the Tycho catalog position (taking into account the proper motion). We derive a CXO coordinate shift of 40 ± 130 mas East, 230 ± 120 mas North from these three tie objects. Since the new WCS for the STIS image is derived from the LCO image, our position for XRF 020427 within the ICRF frame is thus determined to be $\alpha(\text{J2000}) = 22^\text{h}09^\text{m}28^\text{s}.2230$, $\delta(\text{J2000}) = -65°19'32''.031$, with a positional uncertainty of 280 mas ($2\,\sigma$).

We measure the offset of XRF 020427 to be 79 ± 144 mas West, 42 ± 142 mas South ($r = 90 \pm 145$ mas) of the apparent host center; that is, the source position is consistent with the center of the galaxy. The offset corresponds to (0.78 ± 1.25) kpc in projection at a

[4]The predicted and the observed guide star offset differed by 1.678 arcsec, suggesting the absolute pointing and roll angle were systematically incorrect. The culprit was likely the primary guide star (GSC 0912300701 = TYC 2433221), which we calculated from the Tycho-2 catalog had moved 748 mas East, 1148 mas South of the GSC-listed position at the epoch of the HST observation. The approximate magnitude and position angle of the absolute pointing offset was confirmed by observations of WFPC2 parallel images (P.I. S. Casertano; GO/PAR #9318) taken concurrently with the STIS images and eight sources in the USNO A2.0 astrometric catalog. The offset of the Tycho-2 Guide Star from its GSC-listed position is approximately the same as the shift of the native HST WCS relative to the ICRF (see text).

[5]http://www-gsss.stsci.edu/gsc/gsc2/GSC2home.htm

redshift of unity. The localization of the XRF within the host is consistent with, but more accurate than, the results from the same data presented in Fruchter et al. (2003).

4. Properties of the Host Galaxies

The HST photometry of the hosts of both XRF 011030 and XRF 020427 was performed in an aperture of radius 25 drizzled pixels (635 mas). This aperture was selected as a trade off to include as much of the galaxy light without inheriting large errors from an uncertain sky background level. In the NIRC K_s-band image of the field of XRF 011030, we estimated the upper-limit of the host detection by determining the r.m.s. background scatter in a 1.2 arcsec aperture and used an aperture correction determined from a bright unsaturated star.

The host flux of XRF 020427 was found using IRAF/PHOT, with the background level determined from randomly placed apertures in the vicinity of the host. The point spread function of the bright star 5.82 arcsec to the northeast of the host of XRF 011030 cast a faint, but noticeable, increase in the background level around the host galaxy. To remove the contribution of the background to our aperture photometry, we generated 45 independent apertures at the same radial distance from the bright star and computed the total flux in each aperture. We then subtracted the median of the ensemble of these fluxes (after sigma-clipping to remove those apertures with contaminating sources) and estimated the error on the background level by taking the standard deviation of ensemble values.

After a determination of counts per second from the hosts, we converted the instrumental flux to ST magnitudes using the photometry header keywords in the images. We converted the Clear/Longpass colors to the Johnson/Cousins system using template spectra from Bolzonella et al. (2000) redshifted to $z = 0 - 4$. The conversion to the R magnitude is fairly independent of the assumed template and redshift, and the additional uncertainty introduced by the transformation is $\lesssim 0.1$ magnitudes. The transformation to $B - R$ color has a larger uncertainty as it is more sensitive to the assumed template and redshift. The errors in Table 1 include this systematic uncertainty. We note that the ST colors of XRF 011030, *uncorrected* for extinction, are comparable to those derived from the bluest templates of Bolzonella et al. (a star burst spectrum). Therefore the reported $B - R$ should be considered strictly an upper-limit to the true colors. The Galactic extinction toward the fields are $E(B - V)(\mathrm{XRF\,020427}) = 0.029$ mag and $E(B - V)(\mathrm{XRF\,011030}) = 0.393$ mag (Schlegel et al. 1998).

The determinations of magnitudes of the XRF hosts differ from results reported in the literature. Castro-Tirado et al. (2002) reported $R = 23.3 \pm 0.2$ mag and $B = 23.8 \pm 0.4$ mag

for the host XRF 020427 based upon groundbased imaging, brighter by $\sim$1 magnitude than reported herein. However, Castro-Tirado et al. (2002) apparently photometered the entire galaxy complex (within $4'' \times 2''$ region) which was unresolved from the ground, but resolved into three distinct components in HST imaging. We therefore believe that Castro-Tirado et al. (2002) overestimated the host brightness by inclusion of the other nearby galaxies in the aperture. The extinction-corrected magnitude of the host of XRF 011030 reported by Fruchter et al. (2002) is $V \approx 25$ mag. With $V - R = 0.4\,(B - R)$ and $B - R \approx 0.5\,\mathrm{mag}$ we find $V \approx 24.3\,\mathrm{mag}$, a difference of 0.7 mag. The details of the photometry were not given by Fruchter et al. (2002), but the difference could be accounted for by choice of aperture size and the method of determining the background (in the sense that Fruchter et al. 2002 overestimated the background relative to our value). As stated, the presence of the nearby star casts a non-negligible gradient of background light across the host. Both JSB and PGvD photometred the host of XRF,011030 independently, using different background estimators, and found consistent results for the host photometry.

The extinction corrected R-band magnitudes of the XRF hosts give some indication of the probable redshifts. Using the observed GRB host luminosity function (Djorgovski et al. 2003) as an estimator and assuming that XRFs are drawn from the same population of hosts, the redshift median (10%-ile, 90%-ile) of hosts with the same R-band magnitudes of the two XRF hosts is $z = 1.2$ (0.6, 2.6). Interestingly, the color of the host of XRF 020427 cannot be matched by our template galaxy spectra for $z \lesssim 1$. Given no significant drop in flux in the Clear filter from Lyman α absorption, the colors of the host of XRF 020427 suggest that the source originated between a redshift of order unity and $z \approx 3.5$. All of these redshift constraints are relatively insensitive to the unknown intrinsic host galaxy spectral energy distributions. Even with these redshift constraints, we cannot estimate the total energy output of the XRFs as the XRF fluence measurements have yet to be reported.

Visually, the host of XRF 011030 appears as a faint irregular galaxy without a strong central condensation. Because of the overall low signal–to–noise of the object, it is unclear whether a faint feature $\sim$0.64 arcsec southeast from the center is part of the galaxy or an unrelated source. Due to less foreground extinction, the host of XRF 020427 appears brighter than the host of XRF 011030. The XRF 020427 host is asymmetric, which may be the result of a merger or tidal interaction

We fitted two-dimensional exponential and Sérsic morphological profiles to the STIS/Clear images and found that the simplistic profiles are inadequate to fully describe the complex morphologies of the faint hosts. The images are simply not deep enough to properly characterize the shape of the galaxy profiles at large radii. Indeed, as expected, the resulting modeled half-light radii (r_h) depend rather strongly on the assumed profile. Simply taking

the average r_h from our fits and using half of the full range for the error gives $r_h(\text{XRF}\,011030)$ = 560^{+230}_{-140} mas and $r_h(\text{XRF}\,020427) = 300^{+80}_{-70}$ mas. These values correspond to physical sizes of $\sim$2–4 kpc, typical for bulges in the local universe (de Jong 1996).

Irrespective of the assumed profile, the ellipticity of the galaxies is fairly well-constrained: $e(\text{XRF}\,011030) = 0.46 \pm 0.04$ and $e(\text{XRF}\,020427) = 0.72 \pm 0.02$. The position angle (East of North) of the semi-major axes is $32° \pm 2°$ for XRF 020427 and $-44° \pm 4°$ for XRF 011030. As seen in Figure 1, there are two distorted galaxies at comparable magnitudes and colors within a few arcseconds and to the south of the host of XRF 020427, suggestive of a tight grouping of physically related galaxies. No such group is seen in XRF 011030[6].

5. Discussion

To date, four XRFs (011030, 020427, 020903, 030723: Fox et al. 2003) have been followed up reasonably rapidly. In all cases, long-lived lower energy emission, i.e. afterglow emission, appear to have been discovered resulting in sub-arcsecond localizations. For the first two XRFs, we evaluate the probability of chance coincidence of the afterglow positions and a random, unrelated galaxy. Using the offsets, host magnitudes, and the formulation in Bloom et al. (2002), we estimate this chance to be $P_{\text{ch}}(\text{XRF}\,011030) = 0.00797$ and $P_{\text{ch}}(\text{XRF}\,020427) = 0.00595$. Therefore, we believe that, like most other GRBs localized to date, these XRFs are likely to be physically associated with galaxies.

Accepting that these XRFs did indeed occur within their assigned hosts, the photometric evidence presented herein suggests that at least two members of the XRF class cannot be due to GRBs at high redshift. This is consistent with the suggested lack of apparent time dilation between XRFs and GRBs in their respective time histories (Lloyd-Ronning 2002). In addition, the faintness of the hosts (as well as the photometry) suggests both sources occurred with $z \gtrsim 0.6$. This poses difficultly for the original incarnation of the off-axis GRB hypothesis for XRFs (Yamazaki et al. 2002), which require $z \lesssim 0.4$ to be bright enough for detection. Higher maximum XRF redshifts are possible with narrowly beamed jets (Yamazaki et al. 2003), but the GRB collimation angles required ($\lesssim 1°$) do not appear consistent with the inferred distribution of opening angles (Frail et al. 2001).

We can compare the properties of the putative XRF host galaxies to the host galaxies of

---

[6]There are several faint blue galaxies in the field (that are also undetected in K_s-band) at comparable magnitude to the XRF host (e.g., at located at, RA: 20:43:33.49, DEC: +77:17:29.8; 20:43:35.76 +77:17:32.7; J2000). Notably, one such blue galaxy (20:43:35.836, +77:17:21.34) has an arc-like distortion around a red, possibly early-type galaxy, and may therefore be lensed.

GRBs. Adopting the half-light radii as found above, the offsets amount to host-normalized projected offsets of 0.605±0.236 and 0.300 ± 0.490 (XRFs 011030, 020427, respectively) [see Bloom et al. (2002) for a formulation]. Relative to the 20 GRBs in the Bloom et al. sample, the XRFs fall in the 33- and 23-percentile (XRFs 011030, 020427, respectively) in host normalized offset. Since both XRFs are not located at the centers of their respective hosts (as might be expected from an active nucleus origin), from a large-scale perspective, this is tentative evidence that the progenitors of at least some XRFs are related to stellar birthsites.

With an apparent irregular host of XRF 011030 and with the host of XRF 020427 as a possible merger system, morphologically, the XRF hosts are consistent with the diverse sample of GRB hosts (e.g., Bloom et al. 2002). The galaxies associated with GRBs 990123 (Bloom et al. 1999; Fruchter et al. 1999) and GRB 980613 (Hjorth et al. 2002) are examples of disturbed GRB hosts. Photometrically, these XRF hosts appear somewhat brighter than, but not significantly different from, the magnitudes of GRB hosts (e.g., Hogg & Fruchter 1999; Djorgovski et al. 2001; Pian 2001; Sokolov et al. 2001).

While the general consensus is that GRB hosts are a blue, vigorously star-forming population (e.g., Le Floc'h et al. 2003), no strong evidence to date has been published to indicate that they are a population that is significantly different from faint blue galaxies (e.g., Bloom et al. 2001). As blue sources, the hosts of both of these XRFs fit this general trend but until a more complete study has been published on GRB host colors we cannot quantify the extent to which the XRF hosts standout (or fit in). Although the $z \approx 1$ galaxy population has not yet been fully characterized, indications are that a large fraction of galaxies are blue and distorted. Therefore, the XRF hosts may be considered as fairly typical in comparison to the field.

As with GRBs, one would need a larger sample, on the order of a few dozen, to empirically demonstrate any significant link between XRFs and star-forming galaxies. However, the first two well localized host galaxies appear to be similar to those of GRB host galaxies and the prima facie evidence suggest that XRFs, like GRBs, are intimately related to star formation and subsequent stellar death.

Note: After this paper was submitted, Fynbo et al. (2003) placed an upper limit to the redshift of XRF 030723 of $z \approx 2.1$, from the absence of strong Lyman α absorption in the spectrum of the optical afterglow. This confirmed our claim that at least some XRFs do not appear to be a manifestation of GRBs at very high redshift.

REFERENCES

Amati, L. *et al.* 2002, GCN Report 1386

Barraud, C. *et al.* 2003, A&A, 400, 1021

Bloom, J. S. 2003, to appear the Proceedings of "Gamma Ray Bursts in the Afterglow Era, Third Workshop" (Rome, Sept 2002); astro-ph/0303478

Bloom, J. S., Djorgovski, S. G., and Kulkarni, S. R. 2001, ApJ, 554, 678

Bloom, J. S., Kulkarni, S. R., and Djorgovski, S. G. 2002, AJ, 123, 1111

Bloom, J. S. *et al.* 1999, ApJ (*Letters*), 518, L1

Bolzonella, M., Miralles, J.-M., and Pelló, R. 2000, A&A, 363, 476

Castro-Tirado, A. J., Gorosabel, J., Sánchez-Fernández, C., Lund, N., Brandt, S., and Cerón, J. M. C. 2002, GCN Report 1439

de Jong, R. S. 1996, A&A, 313, 45

Dermer, C. D., Chiang, J., and Böttcher, M. 1999, ApJ, 513, 656

Djorgovski, S. G. *et al.* 2001, in Gamma-Ray Bursts in the Afterglow Era, Proceedings of the International workshop held in Rome, CNR headquarters, 17–20 October, 2000, ed. E. Costa, F. Frontera, & J. Hjorth (Berlin Heidelberg: Springer), 218

Djorgovski, S. G. *et al.* 2003, in Discoveries and Research Prospects from 6- to 10-Meter-Class Telescopes II., ed. P. Guhathakurta, Vol. 4834, 238–247

Fox, D. 2002a, GCN Report 1392

—. 2002b, GCN Report 1387

Fox, D. B., Kaplan, D. L., Cenko, B., Kulkarni, S. R., and Nechita, A. 2003, GCN Report 2323

Frail, D. A. *et al.* 2001, ApJ (*Letters*), 562, L55

Fruchter, A. and Hook, R. N. 1997, in Applications of Digital Image Processing XX, Proc. SPIE, Vol. 3164, ed. A. Tescher (SPIE), 120–125

Fruchter, A., Pattel, S., Kouveliotou, C., Rhoads, J., Holland, S., Burud, I., and Wijers, R. 2002, GCN Report 1268

Fruchter, A., Rhoads, J., Burud, I., Levan, A., Patel, S., Kouveliotou, C., Gorosabel, J., and Hjorth, J. 2003, GCN Report 1440

Fruchter, A. *et al.* 1999, ApJ (*Letters*), 519, L13

Fynbo, J. P. U., Hjorth, J., Gorosabel, J., Vreeswijk, P. M., and Rhoads, J. E. 2003, GCN Report 2327

Harrison, F. A., Yost, S., Fox, D., Heise, J., Kulkarni, S. R., Price, P. A., and Berger, E. 2001, GCN Report 1143

Heise, J., in 't Zand, J., and Kulkarni, S. R. 2003, submitted to Nature

Heise, J., in't Zand, J., Kippen, R. M., and Woods, P. M. 2001, in Gamma-ray Bursts in the Afterglow Era, 16

Hjorth, J. *et al.* 2002, ApJ, 576, 113

Hog, E. *et al.* 2000, A&A, 355, L27

Hogg, D. W. and Fruchter, A. 1999, ApJ, 520, 54

in 't Zand, J., Heise, J., Lowes, P., Gandolfi, G., Piro, L., and Costa, E. 2001, GCN Report 1123

in 't Zand, J., Reali, F., Granata, S., Lowes, P., and Piro, L. 2002, GCN Report 1383

Kippen, R. M., Woods, P. M., Heise, J., in't Zand, J., Preece, R. D., and Briggs, M. S. 2001, in Gamma-ray Bursts in the Afterglow Era, 22

Le Floc'h, E. *et al.* 2003, A&A, 400, 499

Lloyd-Ronning, N. M. 2002, to appear in Proc. Woods Hole GRB meeting, Ed. Roland Vanderspek

Matthews, K. and Soifer, B. T. 1994, in Infrared Astronomy with Arrays, the Next Generation, ed. I. McLean (Dordrecht: Kluwer), 239

Mochkovitch, R., Daigne, F., Barraud, C., and Atteia, J. 2003, submitted.

Persson, S. E., Murphy, D. C., Krzeminski, W., Roth, M., and Rieke, M. J. 1998, AJ, 116, 2475

Pian, E. 2001, to appear in "Supernovae and Gamma-Ray Bursters," edited by K. W. Weiler, Springer-Verlag Press

Preece, R. D., Briggs, M. S., Mallozzi, R. S., Pendleton, G. N., Paciesas, W. S., and Band, D. L. 2000, ApJS, 126, 19

Prigozhin, G. *et al.* 2003, GCN Report 2313

Schlegel, D. J., Finkbeiner, D. P., and Davis, M. 1998, ApJ, 500, 525

Soderberg, A. M. *et al.* 2002, GCN Report 1554

Sokolov, V. V. *et al.* 2001, A&A, 372, 438

Taylor, G. B., Frail, D. A., and Kulkarni, S. R. 2001, GCN Report 1136

van Dokkum, P. G. 2001, PASP, 113, 1420

Woosley, S. E., Zhang, W., and Heger, A. 2002, to appear in Proc. Woods Hole GRB meeting, Ed. Roland Vanderspek

Yamazaki, R., Ioka, K., and Nakamura, T. 2002, ApJ (*Letters*), 571, L31

—. 2003, ApJ, in press

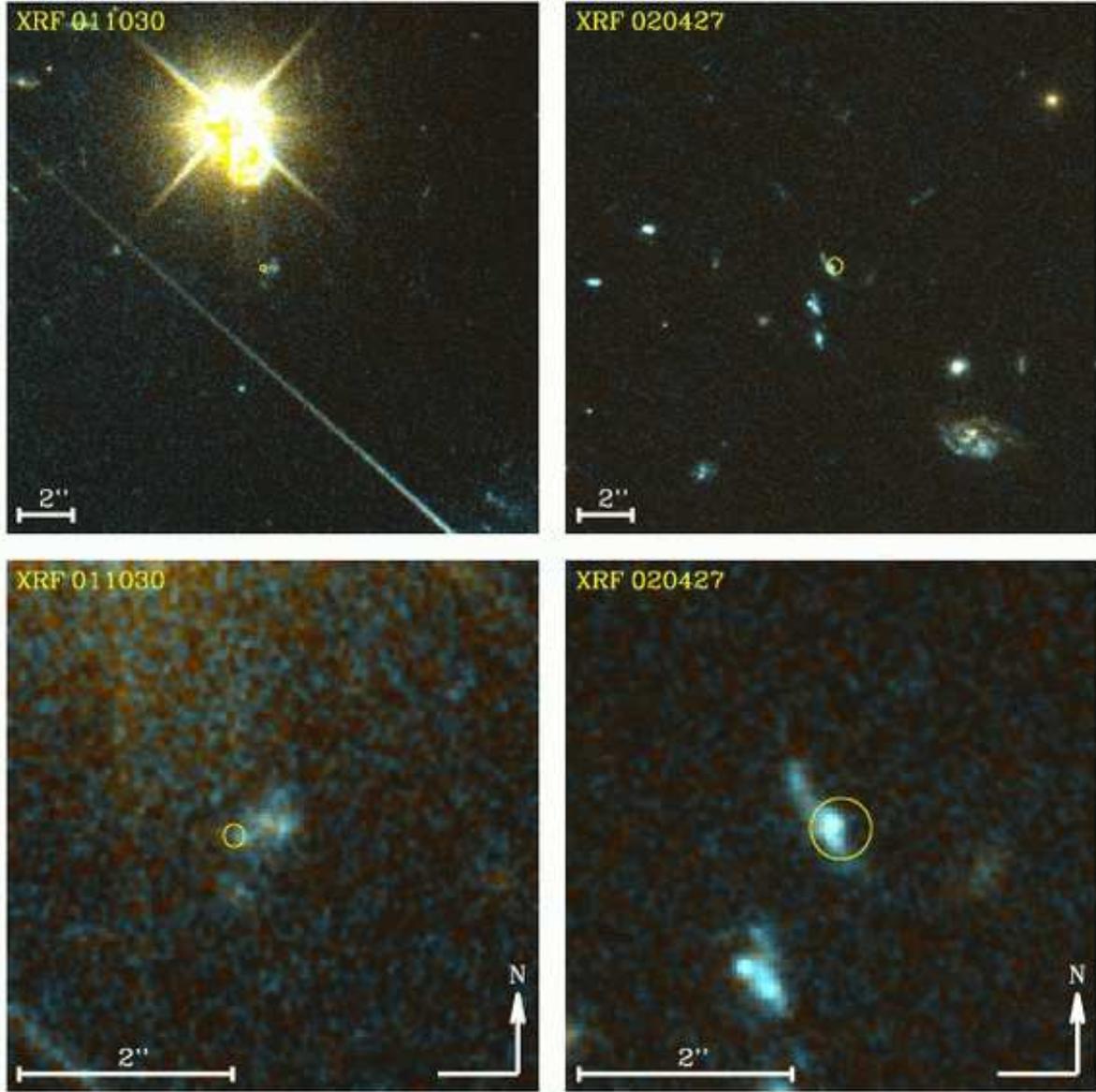Zhang, B. and Mészáros, P. 2002, ApJ, 581, 1236

Fig. 1.— The location and hosts of XRF 011030 and XRF 020427 with false color images constructed from STIS Clear and Longpass observations. Top panels show the 20 × 20 arcsec² field around the XRF positions. Lower panels show the detail of the host regions; ellipses depict the 2-σ position of the XRF from the *Chandra* localization of the afterglows. North is up and East is to the left.

High-resolution version at http://www-cfa.harvard.edu/∼jbloom/xrfs.pdf.

Table 1. Photometry of the Hosts of XRF 011030 and XRF 020427

| Source | Magnitudes[a] | | | | |
	Clear	Clear − Longpass	R_c	$B - R_c$	K_s
XRF 011030 ...	25.24 ± 0.15	0.30 ± 0.29	24.11 ± 0.18	0.6 ± 0.3	>21.70[b]
XRF 020427 ...	24.38 ± 0.05	0.20 ± 0.08	24.23 ± 0.07	0.50 ± 0.15	

[a]The STIS magnitudes are given uncorrected for Galactic extinction. The Johnson magnitudes and errors (cols. 4–5) are given using galaxy templates to match the flux in the STIS filter (see text); these magnitudes have been corrected for Galactic extinction but assume no error in the Galactic extinction value from Schlegel et al. (1998). No correction to the $B - R$ color of XRF 011030 was applied as it is quite dependent on the assumed spectral type and redshift; we note, however, that the *uncorrected* colors are already as blue as the bluest (star burst) template of Bolzonella et al. (2000). The $B - R$ color of XRF 011030 should therefore be considered a strict upper limit. All errors include systematic uncertainties in centroiding and sky subtraction, but assume no error in the STIS zeropoints.

[b]Reported is the 2-σ non-detection limit for the XRF host.